ISSN 1674-1056
http://cpb.iphy.ac.cn
http://iopscience.iop.org/cpb
中国物理 B
Chinese Physics
中国物理 Chinese Physics B

Compact and high-efficient wavelength demultiplexing coupler based on high-index dielectric nanoantennas

Jingfeng Tan(谭敬丰), Hua Pang(庞画), Fengkai Meng(孟凤凯), Jin Jiang(蒋进)

Citation: Chin. Phys. B . 2018, 27(9): 094217. **doi:** 10.1088/1674-1056/27/9/094217

Journal homepage: http://cpb.iphy.ac.cn; http://iopscience.iop.org/cpb

What follows is a list of articles you may be interested in

Coupled resonator-induced transparency on a three-ring resonator

Xinquan Jiao(焦新泉), Haobo Yu(于皓博), Miao Yu(于淼), Chenyang Xue(薛晨阳), Yongfeng Ren(任勇峰)

Chin. Phys. B . 2018, 27(7): 074212. **doi:** 10.1088/1674-1056/27/7/074212

Crosstalk analysis of silicon-on-insulator nanowire-arrayed waveguide grating

Kai-Li Li(李凯丽), Jun-Ming An(安俊明), Jia-Shun Zhang(张家顺), Yue Wang(王玥), Liang-Liang Wang(王亮亮), Jian-Guang Li(李建光), Yuan-Da Wu(吴远大), Xiao-Jie Yin(尹小杰), Xiong-Wei Hu(胡雄伟)

Chin. Phys. B . 2016, 25(12): 124209. **doi:** 10.1088/1674-1056/25/12/124209

Turbulence mitigation scheme based on multiple-user detection in an orbital-angular-momentum multiplexed system

Li Zou(邹丽), Le Wang(王乐), Sheng-Mei Zhao(赵生妹), Han-Wu Chen(陈汉武)

Chin. Phys. B . 2016, 25(11): 114215. **doi:** 10.1088/1674-1056/25/11/114215

Apodized grating coupler using fully-etched nanostructures

Hua Wu(武华), Chong Li(李冲), Zhi-Yong Li(李智勇), Xia Guo(郭霞)

Chin. Phys. B . 2016, 25(8): 084212. **doi:** 10.1088/1674-1056/25/8/084212

X-ray communication based simultaneous communication and ranging

Song Shi-Bin, Xu Lu-Ping, Zhang Hua, Gao Na

Chin. Phys. B . 2015, 24(9): 094215. **doi:** 10.1088/1674-1056/24/9/094215

Compact and high-efficient wavelength demultiplexing coupler based on high-index dielectric nanoantennas*

Jingfeng Tan(谭敬丰)†, Hua Pang(庞画), Fengkai Meng(孟凤凯), and Jin Jiang(蒋进)

State Key Laboratory for Mesoscopic Physics, School of Physics, Peking University, Beijing 100871, *China*

(Received 19 April 2018; revised manuscript received 7 June 2018; published online 28 August 2018)

Wavelength demultiplexing waveguide couplers have important applications in integrated nanophotonic devices. Two of the most important indicators of the quality of a wavelength demultiplexing coupler are coupling efficiency and splitting ratio. In this study, we utilize two asymmetric high-index dielectric nanoantennas directly positioned on top of a silicon-on insulator waveguide to realize a compact wavelength demultiplexing coupler in a communication band, which is based on the interference of the waveguide modes coupled by the two nanoantennas. We add a Au substrate for further increasing the coupling efficiency. This has constructive and destructive influences on the antenna's in-coupling efficiency owing to the Fabry–Perot (FP) resonance in the SiO_2 layer. Therefore, we can realize a wavelength demultiplexing coupler with compact size and high coupling efficiency. This coupler has widespread applications in the areas of wavelength filters, on-chip signal processing, and integrated nanophotonic circuits.

Keywords: wavelength demultiplexing coupler, high-index dielectric nanoantenna, coupling efficiency, Fabry–Perot (FP) resonance

PACS: 42.79.Sz, 42.82.Et, 42.82.–m **DOI:** 10.1088/1674-1056/27/9/094217

1. Introduction

Two of the most important functions of integrated photonic circuits are to couple incident lights efficiently (coupling) and to separate the incident lights with different wavelengths into different directions (demultiplexing).[1] Nanoscale wavelength demultiplexers have several application prospects in color routers, wavelength filters, and on-chip signal processing.[2–5] Extensive approaches have been reported to realize a wavelength demultiplexer using plasmonic components; for example, symmetry-breaking structures such as asymmetric nanoslits, grooves, or nanoantennas,[6–11] multicomponent nanocavities,[12] and cascaded plasmonic nanogratings.[13,14] To realize wavelength demultiplexing by coupling light into dielectric waveguides through nanoantennas is difficult but of considerable importance. Light propagation in dielectric waveguides can diminish the effect of ohmic loss, which is a main problem in plasmonic applications.[15]

In recent years, more attention has been given to the study of the coupling between plasmonics and dielectric photonics,[16–20] which can be utilized to realize directional waveguide couplers or wavelength demultiplexing couplers.[21–26] These devices have the significant advantage of compact size compared to the conventional large-scale optical wavelength demultiplexers based on prisms and gratings.[27,28] For instance, a few plasmonic nanoantennas, such as Yagi–Uda antennas,[22,23] two metal nanoantennas with different sizes,[14,24] an asymmetric V-shape nanoantenna,[25] and a Fano nanoantenna,[5,26] have been reported to realize such a unidirectional or wavelength demultiplexing coupler. However, they have drawbacks including low coupling efficiencies or splitting ratios, which limit their applications. Recently, a novel method based on inverse design has also been reported to realize a high-efficient wavelength demultiplexing grating coupler,[29] however, its feature size is 8 μm. Therefore, it is still a major challenge to realize a compact wavelength demultiplexing coupler with high coupling efficiency and splitting ratio.

In this study, we develop a wavelength demultiplexing coupler based on high-index dielectric nanoantennas, which have recently been proposed as an alternative to plasmonic nanoantennas in the optical regime because of low losses and strong optically induced electric and magnetic resonances.[30,31] We select two asymmetric high-index dielectric nanoantennas because they can couple light into a waveguide more efficiently and provide a strong relative phase difference compared to the plasmonic nanoantennas.[14] When two asymmetric square Si nanoantennas are placed on top of a silicon-on insulator (SOI) waveguide, different resonant properties of the two asymmetric nanoantennas will cause a strong relative phase difference between the waveguide modes coupled by them. A wavelength demultiplexing coupler in a communication band is realized based on the optical interferences of the waveguide modes. A Au substrate is introduced at the bottom of the coupler for further increasing the coupling efficiency. The existence of the Au substrate will have constructive and destructive influences on the in-coupling efficiency of

*Project supported by the National Key Research and Development Program of China (Grant Nos. 2017YFA0205700 and 2015CB932403) and the National Natural Science Foundation of China (Grant Nos. 11174062, 51472057, and 21790364).

†Corresponding author. E-mail: jftan@pku.edu.cn

© 2018 Chinese Physical Society and IOP Publishing Ltd

the antenna owing to the Fabry–Perot (FP) resonance in the SiO_2 layer. As a result, a compact and high-efficient wavelength demultiplexing coupler is obtained, which has important applications in integrated photonic devices.

2. Structure and model

The structure of the wavelength demultiplexing waveguide coupler is schematically depicted in Fig. 1(a). Two high-index square Si nanoantennas are positioned directly on top of an SOI waveguide with a Au substrate. The side lengths of the two square Si antennas are L_1 and L_2, and the distance between them is d. The thicknesses of the Si waveguide and SiO_2 dielectric layer are h and h_1, respectively.

We use the finite-difference time-domain (FDTD) method to examine the coupling and splitting process quantitatively. In the simulation, the permittivity of Au is extracted from experimental data.[32] The refractive index of SiO_2 is set to be 1.45. The data of Palik[33] are used for the permittivity of Si. A Gaussian beam focused to a 3-μm diameter spot with the magnetic component polarized along the y axis (TM) is incident perpendicular to the xoy plane. Two transmission monitors, T_R and T_L, are used to evaluate the power transmitted to the right and left directions in the waveguide, respectively, the sum of which indicates the coupling efficiency of the light incident on the SOI waveguide. The perfect matched layer (PML) boundary condition is used in all directions.

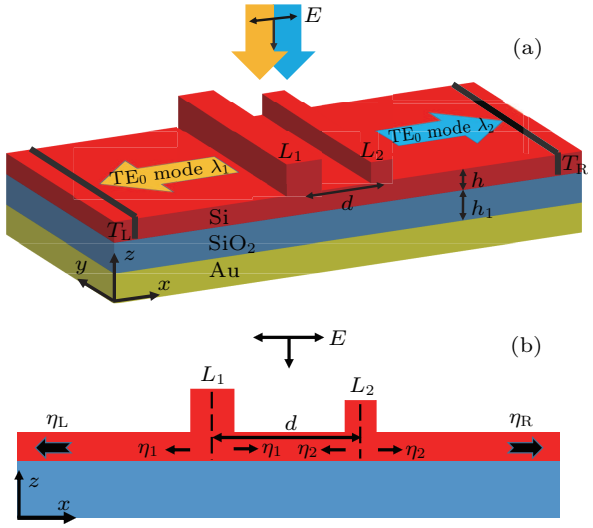


Fig. 1. (color online) (a) 3D schematic diagram of the proposed structure including two high-index nanoantennas on top of an SOI waveguide with a Au substrate. (b) 2D schematic of the designed structure for describing the interference effect of the waveguide modes coupled by the two different nanoantennas.

3. Results and discussion

For simplicity, we first consider two asymmetric high-index square Si nanoantennas placed on top of an SOI waveguide to realize a wavelength demultiplexing coupler. Figure 1(b) shows the schematic of the structure and the mechanism of wavelength demultiplexing. When a p-polarized Gaussian beam illuminates the structure, the two nanoantennas couple the incident light into the waveguide with a phase difference. The amplitudes of the coupled waveguide modes are indicated by η_1 and η_2. The waveguide modes coupled by the two nanoantennas interfere with each other in each direction. When the waveguide modes coupled by one antenna propagate to the counterpart antenna, they will partly transmit through and partly be reflected by the antenna because of the interaction with it. The small reflection is neglected, and the corresponding transmission coefficients are denoted by t_1 and t_2. Then the final amplitudes of the coupled waveguide modes in the right (η_R) and left (η_L) directions are given by

$$\begin{aligned}\eta_R &= \eta_1 \exp\left[\frac{2\pi}{\lambda} n_{\text{eff}} \cdot d + \varphi_1 - \varphi_2 + \Delta\varphi_2\right] t_2 + \eta_2,\\ \eta_L &= \eta_2 \exp\left[\frac{2\pi}{\lambda} n_{\text{eff}} \cdot d + \varphi_2 - \varphi_1 + \Delta\varphi_1\right] t_1 + \eta_1,\end{aligned} \quad (1)$$

where λ is the incident wavelength and n_{eff} is the effective refractive index of the waveguide modes. φ_1 and φ_2 are the initial phases of the waveguide modes coupled by the two different-size nanoantennas; $\Delta\varphi_1$ and $\Delta\varphi_2$ are the phase shifts introduced by the coupled waveguide modes transmitting through antennas L_1 and L_2, respectively. At least two wavelengths must be considered for a wavelength demultiplexer. This implies that the destructive interferences to the right (or left) direction at wavelength λ_1 and to the left (or right) direction at wavelength λ_2 should be realized simultaneously. If $\eta_1 t_2$ equals η_2 and $\eta_2 t_1$ equals η_1, the conditions of the destructive interferences of two wavelengths at opposite directions are

$$\begin{aligned}&\frac{2\pi}{\lambda_1^-} n_{\text{eff}} d + \varphi_1 - \varphi_2 + \Delta\varphi_2 = (2n+1)\pi, \quad n = 0,1,2\ldots,\\ &\frac{2\pi}{\lambda_2^+} n_{\text{eff}} d + \varphi_2 - \varphi_1 + \Delta\varphi_1 = (2m+1)\pi, \quad m = 0,1,2\ldots,\end{aligned} \quad (2)$$

where λ_1^- (or λ_2^+) denotes that the coupled waveguide modes at the incident wavelength of λ_1 (or λ_2) mainly propagate to the left (or right) direction. Thus, we can realize a wavelength demultiplexing coupler in our structure.

We first perform the numerical simulations of individual antennas to better understand the underlying mechanism. The principle of the parameters selecting of the two square Si nanoantennas is to make them have different resonant properties in our research communication band. As a result, the waveguide modes coupled by the two nanoantennas will have a large relative phase difference. Here, the side lengths of the two considered individual square Si nanoantennas are selected as $L_1 = 600$ nm and $L_2 = 400$ nm, and their resonances are magnetic quadrupole (MQ) resonance and electric dipole (ED) resonance in the communication band, respectively. Thus, they can couple incident light into the waveguide

with a large relative phase difference, which is the precondition for realizing a wavelength demultiplexer. Figure 2(a) shows the normalized scattering efficiency of the two isolated nanoantennas excited by a TM plane wave. The electric and magnetic resonances can be clearly observed in the scattering spectrum. The y component of the scattered magnetic fields is shown in Fig. 2(b), corresponding to the MQ resonance at 1460 nm and ED resonance 1360 nm shown in Fig. 2(a). We place the square Si nanoantenna on top of an SOI waveguide with the thickness of Si selected as $h = 250$ nm. When excited by a Gaussian beam focused to a 3-μm diameter spot, the Si nanoantenna couples the incident light efficiently into the waveguide. For instance, for $L_1 = 600$ nm, we find 8% transmission into the fundamental TE mode at one end of the waveguide (16% in both waveguide directions) at the wavelength of 1540 nm owing to the MQ resonance. In addition, for $L_2 = 400$ nm, there is 10% transmission at the wavelength of 1400 nm owing to the ED resonance (Fig. 2(c)). As shown in Fig. 2(d), the waveguide modes coupled by the two antennas have a large relative phase difference in the communication band owing to the different resonant properties (MQ and ED resonances).

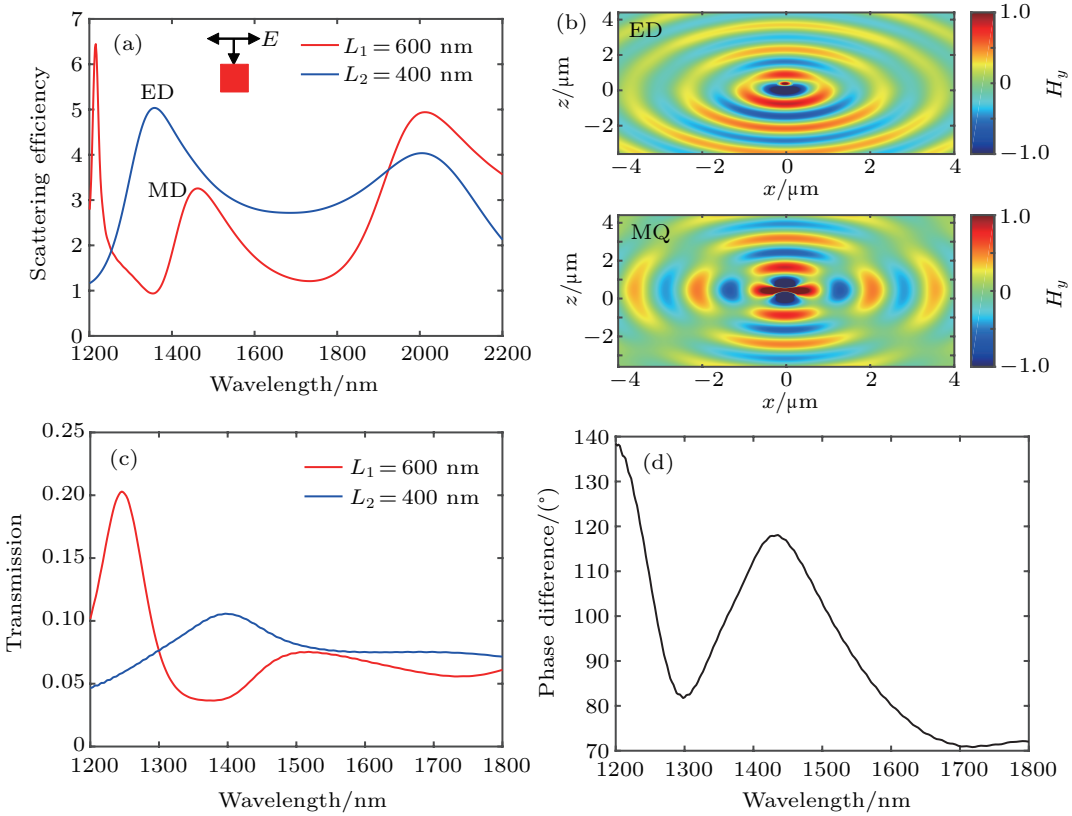


Fig. 2. (color online) (a) Scattering efficiency (defined as ratio of the two-dimensional scattering cross section, which has the dimension of length and geometric length L) of two isolated square Si antennas with side lengths of $L_1 = 600$ nm and $L_2 = 400$ nm. The inset shows the schematic of a Si nanoantenna excited by a TM plane wave. (b) Scattered y component of the magnetic fields of ED resonance at L_2 at the wavelength of 1360 nm and MQ resonance at L_1 at the wavelength of 1460 nm. (c) Transmission to one end of the waveguide for individual L_1 and L_2 excited by a Gaussian beam focused to a 3 μm spot. (d) Relative phase difference between the waveguide modes coupled by the two nanoantennas.

Thus, we can realize a wavelength demultiplexing coupler by placing the two square Si nanoantennas with side lengths of $L_1 = 600$ nm and $L_2 = 400$ nm on the SOI waveguide and varying the distance between them. Figure 3(b) shows the splitting ratio, which is defined as $10\log10(T_R/T_L)$, as a function of the wavelength and the distance between the two nanoantennas. It is clearly observed that the splitting ratio exhibits an oscillation behavior owing to the interference of the waveguide modes coupled by the two antennas (Eq. (2)). As shown in Fig. 3(b), several incident wavelengths can be split in our structure by selecting large antenna spacing. In addition, the two splitting wavelengths and their separation can be easily varied by adjusting distance d. To realize a compact wavelength demultiplexing coupler in the communication band, we select $d = 1290$ nm. Thus, the feature size of our structure is 1.8 μm. As shown in Fig. 3(c), at 1320 nm, the transmission to the right waveguide is 10% with a splitting ratio of 16 dB, whereas at 1510 nm, the transmission to the left waveguide is 14% with a splitting ratio of 17 dB. Figure 3(c) shows the magnitudes of the scattered magnetic fields at wavelengths 1320 nm and 1510 nm in the xoz plane. At 1320 nm, light is only coupled into the fundamental mode of the left waveguide, whereas at 1510 nm, light is only coupled into the right waveguide.

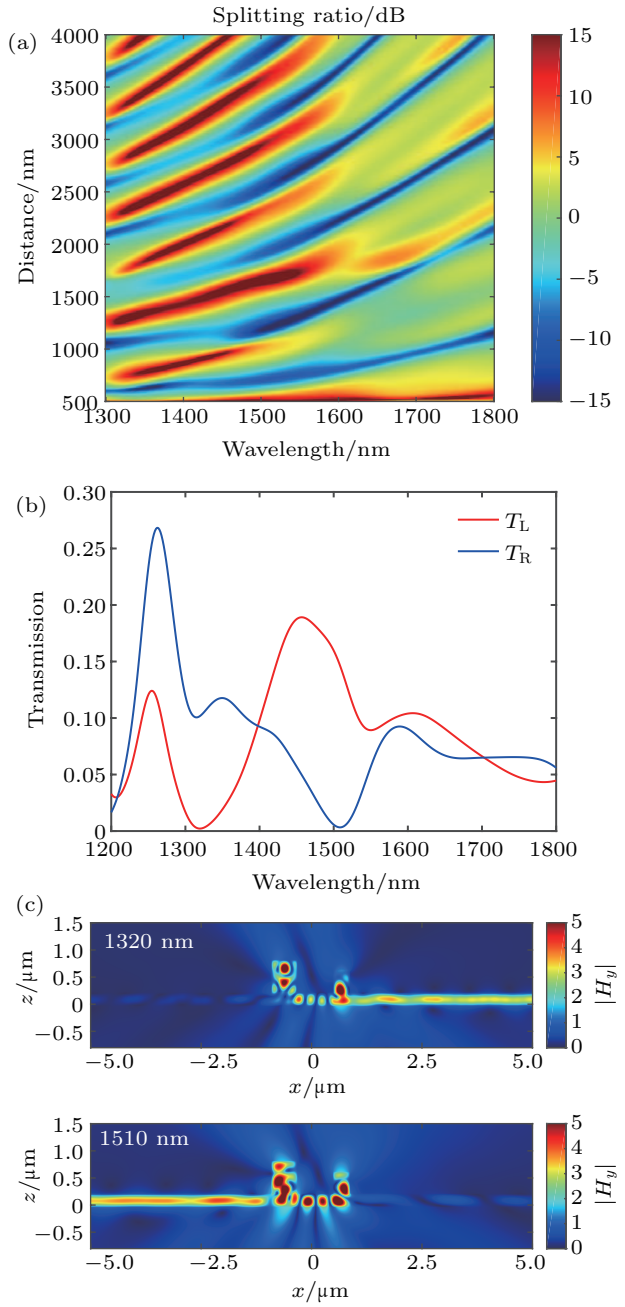


Fig. 3. (color online) (a) Simulated splitting ratio (dB), which is defined as $10\log 10(T_R/T_L)$, as a function of wavelength and the distance between two antennas. (b) Transmission to the right (blue) and left (red) waveguide for the two asymmetric nanoantennas excited by a Gaussian beam focused to a 3 μm spot with distance $d = 1290$ nm. (c) Magnitudes of the scattered magnetic fields at wavelengths 1320 nm and 1510 nm in the *xoz* plane.

A Au substrate is introduced at the bottom of the coupler for further increasing the coupling efficiency. The reflections of the incident light on the Au substrate result in FP resonances in the SiO_2 layer. This leads to wavelength-dependent variations in the field intensity at the antenna's position and produces constructive or destructive influences on the in-coupling efficiency of the antenna. To explain this influence intuitively, we first consider the influence to a single nanoantenna at one wavelength by varying the thickness of the SiO_2 layer, h_1. For example, we consider the antenna with $L_2 = 400$ nm at a wavelength $\lambda = 1400$ nm. Figure 4(b) shows the magnitude of the electric field at the antenna's position (center of the antenna) as a function of thickness h_1 obtained through a simple 1D simulation of the Si/SiO_2/Au stack (Fig. 4(a)). The in-coupling efficiency of the antenna at one end of the waveguide as a function of thickness h_1 is shown in Fig. 4(c). It is clearly observed that the constructive and destructive influences of the electric field intensity at the antenna's position have the same effects on the in-coupling efficiency of the antenna (as shown by the black dashed line).

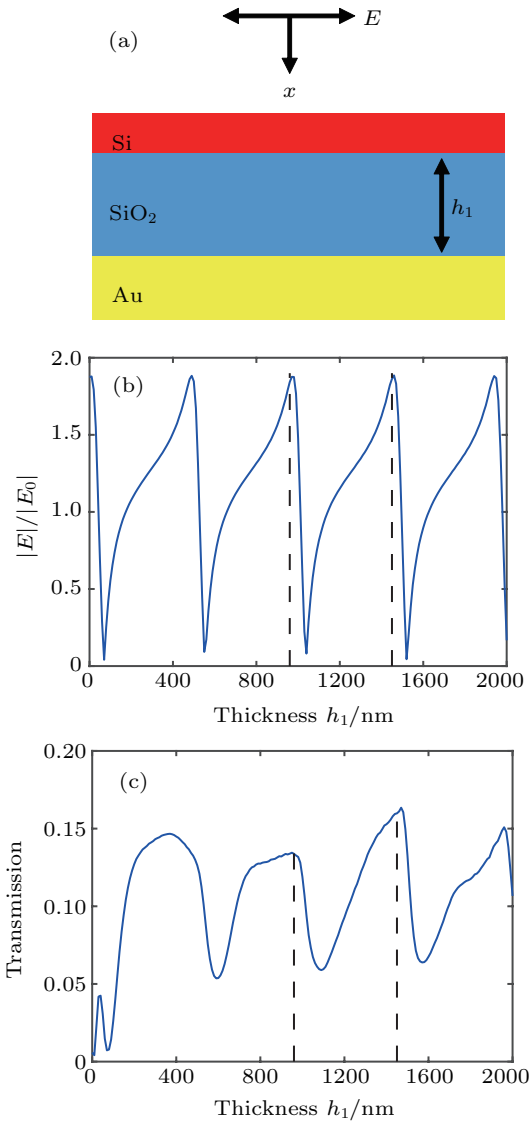


Fig. 4. (color online) (a) Schematic of the Si/ SiO_2 /Au stack. (b) Magnitude of the electric field at the antenna's position (center of the antenna) as a function of thickness h_1 at $\lambda = 1400$ nm. (c) Transmission to one end of the waveguide of the antenna as a function of thickness h_1 at $\lambda = 1400$ nm excited by a Gaussian beam focused to a 3-μm spot.

Therefore, we can further increase the coupling efficiency of the wavelength demultiplexing coupler by adding a Au substrate. The Au substrate is added to the previously designed wavelength demultiplexing coupler, as depicted in Fig. 1(a) with parameters $L_1 = 600$ nm, $L_2 = 400$ nm, $d = 1290$ nm,

and $h = 250$ nm. The existence of the Au substrate first increases the coupling efficiencies of the waveguide modes coupled by the two nanoantennas, then the interference of the waveguide modes results in a wavelength demultiplexing coupler with high coupling efficiency. Figures 5(a) and 5(b) show the transmissions to the right and left waveguides, respectively, as functions of thickness h_1 and wavelength. It can be seen that with the variation in thickness h_1, the transmission to the left waveguide increases considerably between 1400 nm and 1500 nm while the transmission to the right waveguide increases between 1540 nm and 1600 nm. Thus, to realize a wavelength demultiplexing coupler with ultrahigh coupling efficiency, the thickness of the SiO_2 layer is selected as $h_1 = 590$ nm. Figure 5(c) shows the transmissions to the different directions of the waveguide. The splitting ratio is shown in Fig. 5(d). At 1465 nm, the simulated transmission to the left waveguide reaches 41% with a splitting ratio of 30 dB, whereas at 1580 nm, the transmission to the right waveguide is 24% with a splitting ratio of 21 dB. Figure 5(e) shows the magnitudes of the scattered magnetic fields at wavelengths 1465 nm and 1580 nm in the *xoz* plane. Thus, a compact wavelength demultiplexing coupler with high coupling efficiency is realized in our structure.

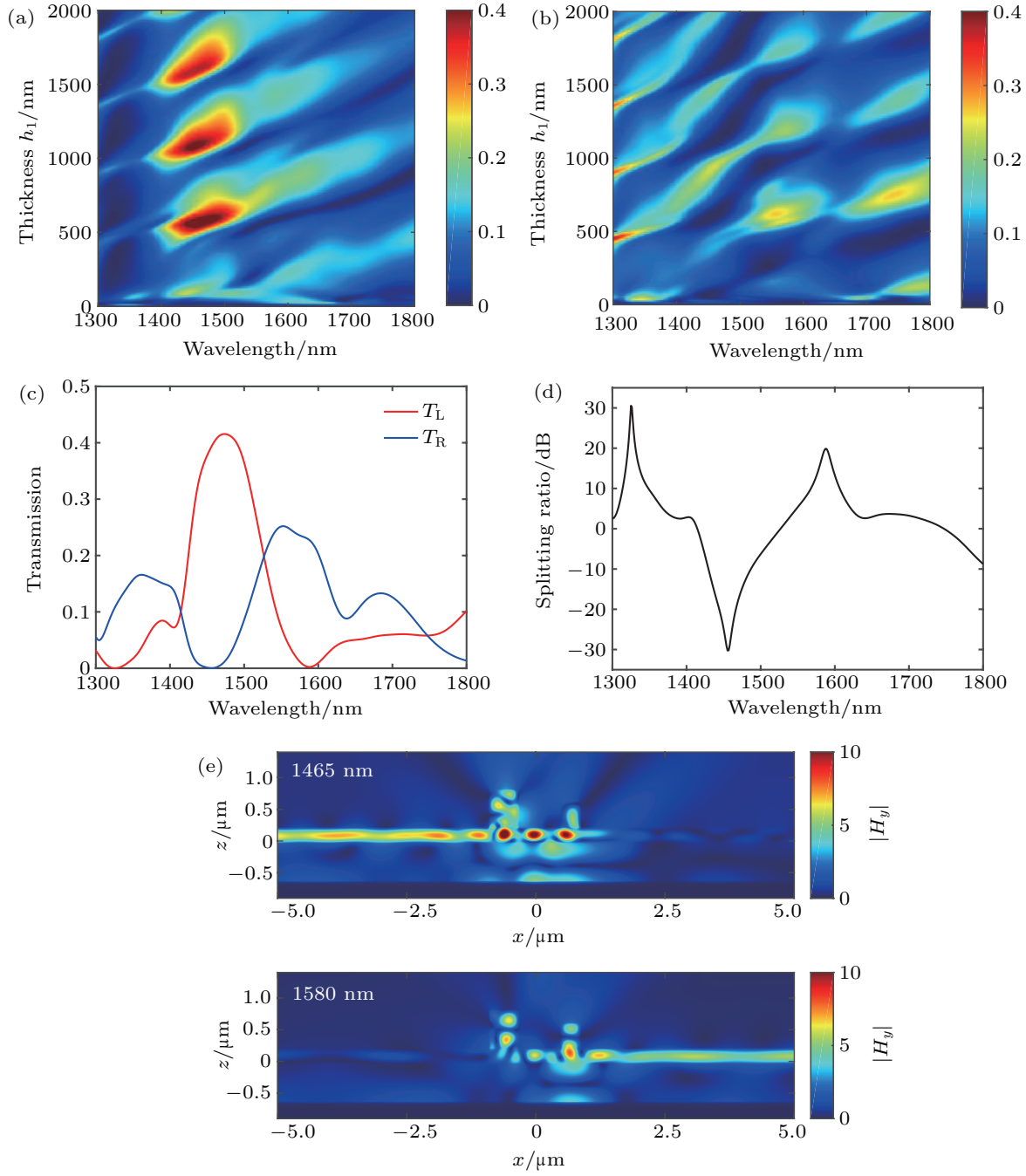


Fig. 5. (color online) (a) Leftward and (b) rightward transmissions in the waveguide as functions of the thickness h_1 and wavelength. (c) Transmission and (d) splitting ratio as functions of wavelength for thickness $h_1 = 590$ nm. The incident Gaussian beam is focused to a 3-μm spot. (e) Magnitudes of scattered magnetic fields at wavelengths 1465 nm and 1580 nm in the *xoz* plane.

Finally, we study the feasibility of the wavelength demultiplexing in our structure in a large spectral region by tuning the geometry parameters. According to the above discussion, the optically induced electric and magnetic resonances of the two high-index dielectric nanoantennas couple vertical incident light into the waveguide with a large relative phase difference. Then, wavelength demultiplexing is realized based on the interference of the waveguide modes coupled by the nanoantennas. As the electric and magnetic resonances of the nanoantennas can be maintained in a large spectral region, wavelength demultiplexing can also be realized in this region. The wavelength demultiplexing coupler in near-infrared and mid-infrared regions with optimized parameters is shown in Fig. 6. The feasibility of the coupler in a large spectral region makes it more attractive for practical applications.

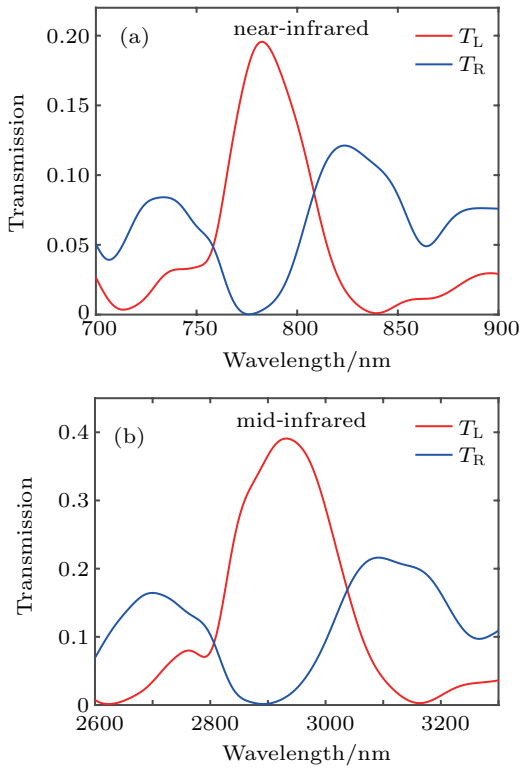


Fig. 6. (color online) (a) Transmission spectra of a wavelength demultiplexing coupler in near-infrared with parameters: $L_1 = 300$ nm, $L_2 = 200$ nm, $d = 700$ nm, $h = 120$ nm, and $h_1 = 310$ nm, Gaussian beam focused to a 2-μm diameter spot. (b) Transmission spectra in mid-infrared with parameters: $L_1 = 1200$ nm, $L_2 = 820$ nm, $d = 2610$ nm, $h = 500$ nm, and $h_1 = 1230$ nm, Gaussian beam focused to a 6-μm diameter spot.

4. Conclusion

We realize a compact wavelength demultiplexing coupler with a feature size of 1.8 μm in a communication band by utilizing two high-index dielectric nanoantennas directly positioned on top of an SOI waveguide. At 1320 nm, the simulated transmission to the right waveguide is 10% with a splitting ratio of 16 dB, whereas at 1510 nm, the transmission to the left waveguide is 14% with a splitting ratio of 17 dB. A Au substrate is introduced at the bottom of the structure for further increasing the coupling efficiency. Thus, we can realize a high-efficient wavelength demultiplexing coupler, for which the transmission to the left waveguide is 41% with a splitting ratio of 29 dB at 1465 nm, and the transmission to the right waveguide is 24% with a splitting ratio of 21 dB at 1580 nm. The splitting wavelengths and their separation can be easily adjusted by tuning the structural parameters. Moreover, this wavelength demultiplexing coupler exhibits feasibility in a large spectral region. Owing to its excellent performance, it has important application prospects in integrated nanoscale photonic devices, such as wavelength filters, color routers, and on-chip signal processing.

References

[1] Piggott A Y, Lu J, Lagoudakis K G, Petykiewicz J, Babinec T M and Vučković J 2015 *Nat. Photon.* **9** 374
[2] Gan Q Q, Guo B S, Song G F, Chen L H, Fu Z, Ding Y J and Bartoli F J 2007 *Appl. Phys. Lett.* **90** 161130
[3] Caglayan H and Ozbay E 2008 *Opt. Express* **16** 19091
[4] Gan Q Q and Bartoli F J 2010 *Opt. Lett.* **35** 4181
[5] Guo R, Decker M, Setzpfandt F, Staude I, Neshev D N and Kivshar Y S 2015 *Nano Lett.* **15** 3324
[6] Liu J S, Pala R A, Afshinmanesh F, Cai W and Brongersma M L 2011 *Nat. Commun.* **2** 525
[7] Sun C W, Chen J J, Li H Y and Gong Q H 2015 *Opt. Lett.* **40** 685
[8] Liao H M, Li Z, Chen J J, Zhang X, Yue S and Gong Q H 2013 *Sci. Rep.* **3** 1918
[9] Zhang X, Li Z, Chen J J, Liao H M, Yue S and Gong Q H 2013 *Appl. Phys. Lett.* **102** 091110
[10] Liu Y M, Palomba S, Park Y, Zentgraf T, Yin X B and Zhang X 2012 *Nano Lett.* **12** 4853
[11] Baron A, Devaux E, Rodier J C, Hugonin J P, Rousseau E, Genet C and Lalanne P 2011 *Nano Lett.* **11** 4207
[12] Lu C C, Liu Y C, Hu X Y, Yang H and Gong Q H 2016 *Sci. Rep.* **6** 27428
[13] Li K, Liu D L, Ho C C, Lu F and Xu A S 2015 *IEEE Photon. Tech. Lett.* **27** 268
[14] Li K, Xiao F, Lu F, Liu D L, Alameh K and Xu A S 2014 *J. Opt. Soc. Am.* B **31** 387
[15] Sidiropoulos T P, Nielsen M P, Roschuk T R, Zayats A V, Maier S A and Oulton R F 2014 *ACS Photon.* **1** 912
[16] Briggs R M, Grandidier J, Burgos S P, Feigenbaum E and Atwater H A 2010 *Nano Lett.* **10** 4851
[17] Alam M Z, Aitchison J S and Mojahedi M 2014 *Laser Photon. Rev.* **8** 394
[18] Guo X, Qiu M, Bao J M, Wiley B J, Yan Q, Zhang X N, Ma Y G, Yu H K and Tong L 2009 *Nano Lett.* **9** 4515
[19] Wen J, Romanov S and Peschel U 2009 *Opt. Express* **17** 5925
[20] Zhang S P, Gu C Z and Xu H X 2014 *Small* **10** 4264
[21] Rodríguez-Fortuño F J, Marino G, Ginzburg P, O'Connor D, Martínez A, Wurtz G A and Zayats A V 2013 *Science* **340** 328
[22] Novotny L and Van Hulst N 2011 *Nat. Photon.* **5** 83
[23] Bernal Arango F, Kwadrin A and Koenderink A F 2012 *ACS Nano* **6** 10156
[24] Sidiropoulos T P H, Maier S A and Oulton R F 2012 *Opt. Express* **20** 12359
[25] Vercruysse D, Neutens P, Lagae L, Verellen N and Van Dorpe P 2017 *ACS Photon.* **4** 1398
[26] Guo R, Decker M, Staude I, Neshev D N and Kivshar Y S 2014 *Appl. Phys. Lett.* **105** 053114
[27] Taillaert D, Van Laere F, Ayre M, Bogaerts W, Van Thourhout D, Bienstman P and Baets R 2006 *Jpn. J. Appl. Phys.* **45** 6071
[28] Roelkens G, Van Thourhout D and Baets R 2007 *Opt. Express* **15** 10091
[29] Piggott A Y, Lu J, Babinec T M, Lagoudakis K G, Petykiewicz J and Vučković J 2015 *Sci. Rep.* **4** 7210
[30] Aieta F, Kats M A Genevet P and Capasso F 2015 *Science* **347** 1342
[31] Kuznetsov A I, Miroshnichenko A E, Brongersma M L, Kivshar Y S and Luk'yanchuk B 2016 *Science* **354** 2472
[32] Johnson P B, Christy R W 1972 *Phys. Rev. B* **6** 4370
[33] Palik E D 1985 *Handbook of Optical Constants of Solids* (New York: Academic Press)